Chemical Engineering Journal 150 (2009) 431–439

Contents lists available at ScienceDirect

Chemical Engineering Journal

journal homepage: www.elsevier.com/locate/cej

Effect of operating conditions on iron corrosion rates in zero-valent iron systems for arsenic removal

Juan M. Triszcz[a], Andrés Porta[a,b], Fernando S. García Einschlag[c,*]

[a] Laboratorio de Ingeniería Sanitaria (LIS), Departamento de Hidráulica, Facultad de Ingeniería, Universidad Nacional de La Plata, 48 e/115 y 116, CP (1900), Argentina
[b] División Química Analítica, Departamento de Química, Facultad de Ciencias Exactas, Universidad Nacional de La Plata, 47 y 115, CP (1900), Argentina
[c] Instituto de Investigaciones Fisicoquímicas Teóricas y Aplicadas (INIFTA), CCT-La Plata-CONICET, Departamento de Química, Facultad de Ciencias Exactas, Universidad Nacional de La Plata, 64 Diag. 113, CP (1900), Argentina

ARTICLE INFO

Article history:
Received 19 September 2008
Received in revised form
26 December 2008
Accepted 19 January 2009

Keywords:
Arsenic removal
ZVI
Iron corrosion

ABSTRACT

Owing to newly established water quality standards, the use of the zero-valent iron (ZVI) method for arsenic removal is gaining attention. The spontaneous chemical oxidation of ZVI by dissolved oxygen, a complex process involving a variety of metastable ferrous–ferric intermediate species, was studied in short-term batch experiments using two different commercially available ZVI materials. Differences in corrosion rates may be attributed to the different specific reactivity of these materials. The effects of pH, ZVI loading, initial conductivity and dissolved oxygen concentration on both Fe(II) and Fe(III) kinetic profiles were investigated. ZVI corrosion rates in the presence of As(III) and As(V) were also studied. Depending on the pH, the concentrations of Fe(II) and Fe(III) are significantly influenced by the presence of As(III) and As(V). Our results may be important from a technological point of view, since it is well known that iron corrosion rates govern the generation of sites for arsenic removal.

1. Introduction

The presence of arsenic compounds in groundwater, one of the main sources of drinking water, is a serious environmental and health problem. Increased concentrations of arsenic in natural waters have been reported in many regions of the world. The predominant oxidation states of inorganic arsenic in water are As(III) and As(V). The pH of most natural waters lies between 5 and 9, the important As species being $H_2AsO_4^-$, $HAsO_4^{-2}$ and H_3AsO_3 [1,2]. As(III) is more mobile and more toxic than As(V). Long-term exposure to high levels of arsenic in drinking water may cause skin alteration, damage to major body organs and many types of cancer.

Several techniques have been proposed for arsenic removal from water. Current technologies include precipitation, coagulation and filtration, reverse osmosis, electrodialysis, ion exchange and adsorption.

In recent years, the zero-valent iron (ZVI) method for the in situ remediation of groundwater has gained considerable interest [4,5,26,33,35]. The detoxification effectiveness, low cost, and benign environmental impact of Fe(0) facilitate the development of water treatment processes, and several studies [4,5,20,24,25] have demonstrated that ZVI effectively reduces the concentration of several organic and inorganic pollutants. In particular, the ZVI method has also been intensively studied due to its ability to remove arsenic compounds [2,4–11] and has been successfully applied for groundwater remediation. In comparison with other methods, ZVI can simultaneously remove As(V) and As(III) without previous oxidative treatment and does not require the use of additional chemical products, since metallic iron is used for the sustained production of colloidal hydrous ferric oxides (HFO) [5,9].

The mechanism of arsenic removal by ZVI is rather complex since different processes are involved. It is generally accepted that As uptake from aqueous systems at near neutral pH is based on adsorption and co-precipitation phenomena coupled with the continuous generation of iron oxyhydroxides [7,10]. Several spectroscopic and electrochemical studies have confirmed the strong interaction among ZVI-corroded surfaces and inorganic arsenic species [4,8,11]. However, depending on the operating conditions different processes, such as redox reactions associated with iron corrosion and arsenic speciation, co-precipitation and adsorption, may have an important role in controlling the overall effectiveness of arsenic removal. Therefore, in order to gain a better understanding of the overall uptake mechanism, it is desirable to analyze in detail the effect of key variables, such as pH and dissolved oxygen concentration, on each one of the individual processes.

The spontaneous chemical oxidation of ZVI in the presence of dissolved oxygen (i.e., corrosion) is a complex process involving a variety of metastable ferrous–ferric intermediate species, which are

* Corresponding author at: INIFTA, Universidad Nacional de La Plata, Diagonal 113 y 64, Casilla de Correo 16 Sucursal 4, Código Postal 1900, La Plata, Argentina. Tel.: +54 221 425 7291/425 7430; fax: +54 221 425 4642.
E-mail address: fgarciae@quimica.unlp.edu.ar (F.S.G. Einschlag).

1385-8947/$ – see front matter © 2009 Elsevier B.V. All rights reserved.
doi:10.1016/j.cej.2009.01.029

ultimately transformed into different stable iron oxides. It is known that Fe(II), which is the primary product of ZVI oxidation, may stay at the interface, where it may either form ferrous precipitates (i.e., carbonate, hydroxide, etc.) or oxidize further; or may be transported away from the surface, where it is subject to homogeneous oxidation and precipitation of Fe(III) [3,5,14,34]. Many research groups have discussed the stratified nature of the corrosion coating formed on the metallic iron surface that, depending on the reaction conditions, involve different stable and metastable phases of iron oxides [7,12,13]. Moreover, Fe(III) can be reduced to Fe(II) by Fe(0), especially in oxygen-depleted environments where this heterogeneous autoreduction reaction is a potentially important process for ZVI systems [12]. However, it has also been reported that aerobic and high ionic strength conditions are likely to promote the formation of Fe(III) colloidal species away from the Fe(0) surface [19,20].

In spite of the physicochemical complexity associated with the removal of arsenic in ZVI systems, reactions 1–6 [2,5,6,35] roughly represent the most relevant processes that may be involved in the formation of iron species associated with As uptake at circumneutral pH.

$$Fe(0) + 2H_2O \rightarrow Fe(II) + H_2 + 2HO^- \quad (R1)$$

$$Fe(0) + H_2O + 1/2O_2 \rightarrow Fe(II) + 2HO^- \quad (R2)$$

$$Fe(0) + 2Fe(III) \rightarrow 3Fe(II) \quad (R3)$$

$$Fe(II) + 1/2H_2O + 1/4O_2 \rightarrow Fe(III) + HO^- \quad (R4)$$

$$Fe(III) + 3H_2O \rightarrow Fe(HO)_3 + 3H^+ \quad (R5)$$

$$Fe(II) + CO_3{}^{-2}/HO^- \rightarrow \text{ferrous precipitates} \quad (R6)$$

The kinetics of Fe(0) oxidation as well as the sorption properties of iron corrosion products can be strongly affected by the operating conditions, and some aspects concerning the relative contribution of (R1)–(R6) to the mechanism of ZVI corrosion have not been completely clarified. This poses a serious disadvantage for the development of efficient treatment facilities, since corrosion rates are closely related to the kinetics of arsenic uptake [4,7]. In addition, most studies have focused on arsenic removal and the characterization of the oxide coating on the Fe(0) surface, but only a few researchers [5,6,19,20] have addressed the behavior of soluble and colloidal iron. Given that column tests [6,21] have shown an inverse correlation between effluent concentrations of arsenic and iron, the investigation of suspended iron species is a key issue for reactor design purposes.

Since both the production rates and the distribution of iron particles are critical factors affecting arsenic removal, we focused our efforts on the characterization of the suspensions resulting from ZVI corrosion. The aim of the present work was to study the influence of different variables, such as metal/aqueous phase contact area, solution conductivity, pH, dissolved oxygen concentration and the presence of arsenic species, on the production kinetics of soluble and colloidal iron species. The particular approach adopted is useful for assessing the partial contribution of iron corrosion rates to the overall mechanism of arsenic removal.

2. Materials and methods

2.1. Materials

Analytic grade NaCl (99.5%), $CaCl_2$ (99.0%), $FeSO_4{\cdot}7H_2O$ (>99.0%), $MgCl_2{\cdot}6H_2O$ (99.0%) and NaOH (>97.0%) were supplied by Riedel-de Haën; $NaHCO_3$ (>99.7%), $NaNO_3$ (>98.0%) and HCl (36.5–38.0%) were purchased from Merck, and Na_2SO_4 (>99.0%) supplied by Sigma; they were all used as received. Stock solutions were prepared using deionized water (<3 μS/cm). Stock solutions containing 1000 mg/L of As(III) or As(V) were prepared from reagent-grade As_2O_3 (>99.0%, Merck) and $Na_2HAsO_4.7H_2O$ (>98.5%, Sigma), respectively. Nitrogen, oxygen and analytic air were supplied by AGA.

Two commercially available iron-based materials were used, without previous treatment, as ZVI sources: lost head iron nails (EGA® 8–25: C % <0.03, Mn % 0.20–0.30, S % <0.025, P % <0.025, Si % <0.05) and steel wool (Mapavirulana®: C % 0.076–0.84, P % 0.015–0.018, S % 0.011–0.014, Mn % 0.810–0.86, Si % 0.115–0.146). Specific surface areas, determined by N_2 adsorption at −195.8 °C (BET method) using a Micromeritics ASAP 2020 instrument, were 0.80 ± 0.07 and $2.02 \pm 0.09\ m^2/g$ for the lost head nails and steel wool, respectively.

2.2. Experimental setup and conditions

Batch experiments were conducted in a 500-mL cylindrical glass reactor at 21 ± 1 °C in the dark. The reactor was equipped with a manifold for gas bubbling and a lateral sampling port. ZVI samples were placed at the bottom in direct contact with the gas inlet. The pH, pO_2 and conductivity were continuously recorded. Vigorous stirring was performed using a magnetic bar at 300 rpm. At different periods of mixing time, representative samples of 10-mL were withdrawn from the center of the reactor by a Teflon tube connected to a plastic syringe. Most of the experiments were performed in the presence of oxygen under continuous air purging. Unless otherwise stated, an air flow rate of 0.8 L/min was used.

The working solutions were prepared using either tap water from La Plata or a synthetic aqueous matrix of well-known composition (Table S1, Sup. Mat.). For the experiments presented in Section 3.3, the solutions were prepared using deionized water. Different amounts of 1000 mg/L solutions of NaCl, $NaNO_3$ or Na_2SO_4 were employed in order to set the conductivity to desired values. Stock solutions of 1 g Na_3AsO_4/L and 1 g As_2O_3/L were used to adjust arsenic concentrations for the experiments shown in Section 3.6. In all cases, before starting the experiments, solutions were purged with air (or N_2 for the tests conducted in the absence of oxygen) for 30 min. Then, the initial pH was adjusted to the desired value using HCl or NaOH; however, the pH was not controlled during the course of the experiments.

2.3. Analysis

In order to characterize the production of suspended and soluble iron species we used two operationally defined fractions, namely "total" and "filterable" iron based on physical separation through 0.45 μm syringe filters [2,15]. Although we recognize that the filterable fraction includes not only soluble iron but also colloidal particles of amorphous oxyhydroxides capable of passing through the nylon filter, the operational definition is useful from an engineering viewpoint. Thus "total Fe(II)" ($Fe(II)_{tot}$) and "total Fe(III)" ($Fe(III)_{tot}$) concentrations were obtained by sampling the working suspensions and acidifying them with concentrated HCl to dissolve any suspended precipitates before the analysis. On the other hand, "filterable Fe(II)" ($Fe(II)_{filt}$) and "filterable Fe(III)" ($Fe(III)_{filt}$) concentrations were measured by passing the samples through plastic filters (Whatman, 25 mm GD/X Syringe Filters, 0.45 μm) before the addition of HCl in order to retain nonfilterable particles. The concentrations of Fe(III) and Fe(II) in the acidified samples were quantified by spectrophotometry, through the complexes formed with KSCN and *o*-phenantroline, respectively, as described elsewhere [22].

Quantitative determination of arsenic concentrations was performed by applying the silver dithiodiethylcarbamate standardized method [23], before analysis samples were filtered through the aforementioned plastic filters. All analytic data were assessed for accuracy and precision using a quality control system involving

duplicates, blanks and standard samples during the analytical procedure.

Physicochemical analyses of the drinking water used to prepare the working solutions were conducted according to the following standardized techniques: conductivity (HANNA Instruments, HI 9033); fluoride (Orion, model 96-04 ionalizer); nitrate (Orion, model 9707 ionplus); sulfate (nefelometry, Hach 2001); chloride (argentometer method); hardness (titrimetric method with EDTA); and nitrite (Llosva von llosva method). The pH was determined by using a pH electrode (HANNA Instruments, model 8521/Orion 720), whereas dissolved oxygen concentrations were recorded with a selective electrode (Orion, model 850A+/083005D).

3. Results and discussion

3.1. Effect of dissolved oxygen concentration

3.1.1. Corrosion kinetics and iron oxidation states

Batch experiments were carried out in order to characterize the formation of different iron corrosion products with different dissolved oxygen concentrations. Steel wool was used as ZVI source. The concentration profiles were tracked during the first 60 min since preliminary corrosion and adsorption experiments, performed in our laboratory in air-saturated vessels for at least 8 h, showed that iron species attain a stationary state during the first 30 min, whereas arsenic concentrations reach a 90% of their sorption equilibrium values within 60 min. For the experiments conducted in the absence of oxygen, no change in pH was recorded. On the other hand, during the aerated tests pH shifts of less than one unit were observed during the first 15 min, then the pH remained constant.

In the absence of dissolved oxygen, a negligible production of suspended and soluble iron species was observed during the analyzed timescale (Section 3.5.1), whereas the results presented in Fig. 1 show that the oxygen concentration has a decisive effect on both the rates of formation and the oxidation states of suspended and soluble iron species. The experiments conducted under continuous air supply showed that filterable iron reaches a steady value after the first 10–20 min and that $Fe(III)_{tot}$ increases linearly with time (Fig. 1a), whereas the experiments performed in closed vessels showed a first-order kinetic law for the consumption of dissolved oxygen (Fig. 1b); both results are in agreement with previous studies [2,24].

Interestingly, during the analyzed timescales, no visible corrosion coating was observed on the steel wool surface for the experiments performed under continuous air supply. Although we cannot completely rule out the formation of a corrosion layer of increasing thickness onto the ZVI surface, the absence of visible changes on the steel wool, together with the observation and quantification of considerable amounts of suspended particles through $Fe(II)_{tot}$ and $Fe(III)_{tot}$ measurements, suggests that the amount of corroded iron attached to the steel wool surface is of minor importance under our experimental conditions.

It is worth mentioning that for the experiments performed in closed reaction vessels, the corrosion products evolved with time since the initial colorless solution became yellow during the first minutes and the colors of the precipitates (obtained by sedimentation in Imhoff cones) changed from reddish, for oxygen-saturated suspensions, to dark brownish and finally to black when the dissolved oxygen was depleted. Although a structural analysis of the solid particles is beyond the scope of our work, direct inspection of the observed precipitates suggested a shift from particles containing mostly Fe(III) to particles containing a mixture of Fe(II) and Fe(III) as dissolved oxygen diminished, which is in good agreement with previous studies [3,16,24,25]. This result may be ascribed to the reduction of Fe(III) by ZVI (R3), which is likely to play an important role in oxygen-restricted environments [12].

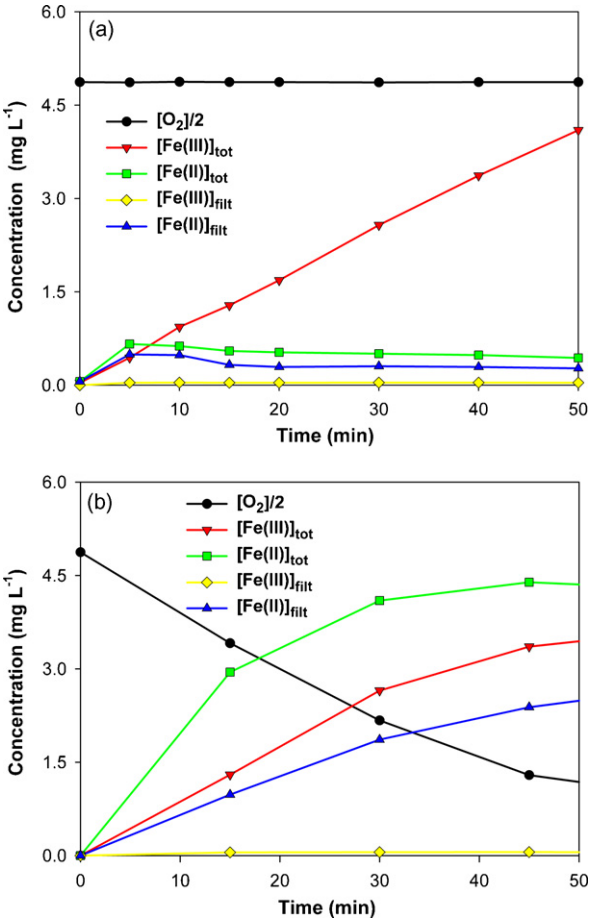

Fig. 1. Concentration profiles of oxygen and iron species in the working suspensions: (a) continuous air purging at 0.8 L/min; (b) closed vessel initially saturated with air. Conditions: tap water; σ_{ini} = 820 μS/cm; pH_{ini} = 7.1; $m_{steel\ wool}$ = 3 g/L.

The simultaneous analysis of the oxidation states observed for total and filterable iron fractions allows drawing useful conclusions concerning the corrosion mechanism under different conditions. Total Fe(III) profiles show that the amount of ferric species produced in air-saturated suspensions increases linearly with time (Fig. 1a). On the other hand, when the availability of dissolved oxygen is limited (Fig. 1b), the production rate of suspended Fe(III) species decreases and becomes negligible under anoxic conditions. Besides, the amounts of Fe(II) species in air-saturated solutions are lower than the ones observed under oxygen-restricted conditions. The increase in the $Fe(III)_{tot}/Fe(II)_{tot}$ ratio observed for the air-saturated tests is associated with the oxidation of Fe(II) species to Fe(III) species by dissolved oxygen (R4), which is known to occur relatively fast under neutral and basic conditions [17,18]. These results show that suspended particle generation is connected to dissolved oxygen consumption.

The formation of ferric species from zero-valent iron involves two consecutive processes. During the first stage, metallic iron is oxidized to ferrous iron by heterogeneous reactions, whereas the second stage involves the oxidation of ferrous ions to ferric ions (R4), which can be both homogeneous and heterogeneous [17,34]. The experiments performed under air saturation suggest that Fe(II) profiles quickly achieve relatively low steady values where ferrous species production and consumption rates are equated. This behavior, which was observed for all the conditions tested provided that oxygen was continuously supplied, can be explained taking into

account that R4 follows first-order kinetics with respect to both [O_2] and [Fe(II)] and displays a high rate constant at circumneutral pH values [18]. Consequently, our results indicate that the oxidation of zero-valent iron to yield ferrous species is the rate-controlling step of corrosion product formation.

3.1.2. Enhancement of ZVI reactivity by Fe(II)

The comparison of the kinetic profiles observed for Fe(II) (Fig. 1) reveals that larger amounts of Fe(II) are detected for low dissolved oxygen concentrations. This behavior is partially related to the increase of Fe(II) lifetime for the oxygen-limited experiment since Fe(II) oxidation rates are proportional to the concentration of dissolved oxygen.

In addition, it is also worth pointing out that the analysis of apparent ZVI corrosion rates suggests that the oxidation of metallic iron is faster for the oxygen-limited experiment. Therefore, in order to test the effect of Fe(II) concentration on ZVI corrosion rates, we performed a set of experiments using different initial Fe(II) concentrations (Fig. S1, Sup. Mat.). After 60 min, the experiments started without adding Fe(II) and with initial additions of 0, 3.9 and 5.9 mg/L Fe(II) showed $[Fe(II)]_{total}$ values of 4.5, 9.6 and 12.6 mg/L, respectively. These results show that the reactivity of steel wool is somewhat enhanced in the presence of ferrous species, a behavior that has already been reported in previous studies involving zero-valent iron [24,25]. The mechanism whereby iron corrosion caused by dissolved oxygen is accelerated by the presence of Fe(II) has been discussed by Huang and Zhang [25]. They proposed that the enhanced reactivity of Fe(0) is related to the adsorption of Fe(II) on the corrosion coating formed on the ZVI surface. Thus, adsorbed Fe(II) is believed to facilitate the electron transfer between oxygen and metallic iron that is otherwise shielded by the corrosion coating.

The results presented in Sections 3.1.1 and 3.1.2 indicate that the higher $Fe(II)_{tot}$ values recorded during the experiments conducted under oxygen-restricted conditions (Fig. 1b) may be related to the following issues: (i) the decrease in Fe(II) consumption due to the unavailability of dissolved oxygen, (ii) the relative increase in the reduction of Fe(III) by ZVI and (iii) the increase in Fe(II) production due to the enhanced ZVI oxidation at higher [Fe(II)]. Since both iron corrosion rates and arsenic oxidation states may be influenced by the concentrations of Fe(II) and oxygen [7,9], and considering that [Fe(II)] is strongly dependent on [O_2], the availability of dissolved oxygen is a key parameter for the design of efficient treatment facilities due to its complex relationship with both the rates and the mechanism of arsenic removal.

3.1.3. Oxygen transport to the ZVI/solution interface

In order to ascertain the effect of the oxygen supply rate on $Fe(III)_{tot}$ production, batch tests were performed varying the air flow rate from 0.10 to 0.80 L/min. The production rate of $Fe(III)_{tot}$ was practically independent of air bubbling for flow rates larger than 0.42 L/min. Nevertheless, for lower air supply rates, there was a strong inhibition of total $Fe(III)_{tot}$ generation. This result confirms that dissolved oxygen concentration plays a key role in the overall process.

An additional test was conducted with the aim of characterizing the transport of dissolved oxygen to the ZVI/solution interface. The steel wool was placed inside the reactor and, after bubbling with an air flow rate of 0.8 L/min for 2 h, the air supply was interrupted. Then the system open to the atmosphere was unperturbed for 24 h. The resulting distribution of dissolved oxygen was determined by a pO_2 selective electrode (Fig. S2, Sup. Mat.) and shows that a concentration gradient of O_2 is produced inside the batch reactor owing to oxygen consumption and mass transfer limitations. The lowest pO_2 values were observed in the ZVI neighborhood, indicating a local O_2 consumption due to the oxidation of ZVI and some of its corrosion products. On the other hand, the largest pO_2 values were observed near the air/solution interface due to diffusion of atmospheric oxygen into the reactor.

Mass transfer limitations for arsenic species adsorption onto iron oxide surfaces have already been discussed [7,21,36]. Additionally, our results show that the inhomogeneous distribution of dissolved oxygen may also be important from a technological perspective since the transport of O_2 through the diffusion layer may have a critical impact on iron corrosion rates.

3.2. Effect of ZVI exposed area

A comparative study of the $Fe(III)_{tot}$ generation rates was performed using different loadings of lost head nails or steel wool. The pH and conductivity of the solutions showed slight increases during the first 15 min, and then constant values were recorded. It should be pointed out here that, unlike in steel wool, in lost head nails there were visible corrosion products on the ZVI surface and the initial metallic glaze faded with time.

The results presented in Fig. 2 show that the rates of corrosion product generation are intimately related to the contact area for both ZVI sources. However, for contact areas smaller than 5 m^2, the corrosion rates in steel wool are about 10 times larger than in lost head nails, indicating that the steel wool surface is much more reactive than the surface of lost head nails. These results are in line with the studies reported by Su and Puls [4], who found that arsenic removal efficiencies are not uniquely correlated with the exposed ZVI area. It should be noted that many factors such as Fe(0) composition, surface properties, mechanical abrasion and the nature of the iron oxide coating may influence the reactivity of ZVI [4,12,24].

In addition, within the analyzed range, the rates of Fe(III) production recorded with lost head nails are linearly dependent on the area of ZVI employed, further suggesting that the overall corrosion rate is controlled by the initial heterogeneous stages of metallic iron oxidation. On the other hand, the tests made with commercial steel wool show a more complex dependence, since total Fe(III) formation rates reach a maximum for contact areas close to 6 m^2 and then slightly decrease for larger iron loadings. Thus, although the exposed area may be a decisive factor in the kinetics of iron oxidation, the absence of linearity observed in the tests with steel wool suggests that for large contact areas other factors may limit the rate of ferric species formation. In particular, the latter behavior could be related to the decrease of the ratio $Fe(III)_{tot}/Fe(II)_{tot}$ expected for the low dissolved oxygen concentration at the ZVI/suspension interface due to mass transfer limitations discussed in Section 3.1.3. From

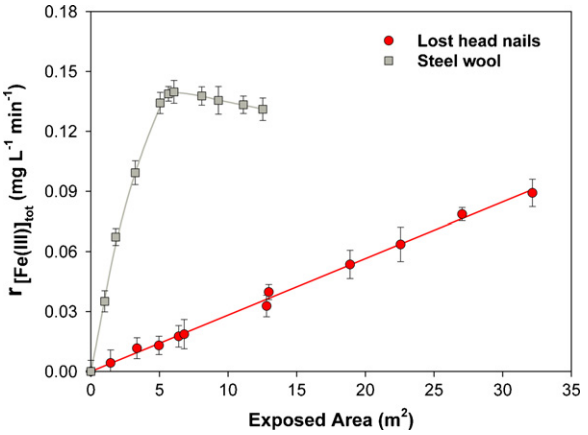

Fig. 2. Effect of exposed surface BET-area on $Fe(III)_{tot}$ production rates. Conditions: synthetic water; σ_{ini} = 1500 μS/cm; pH_{ini} = 7.0; air flow = 0.8 L/min; $m_{steel\ wool}$ = 0–5 g/L; $m_{lost\ head\ nails}$ = 0–40 g/L.

Table 1
[$Fe(III)_{tot}$] production rates at different initial conductivities[a].

Salt	Conc. (g/L)	σ_{ini} (mS/cm)	$r_{steady,Fe(III)tot}$ (mg/L min)[b]	pH_{steady}
NaCl	0.99	2.72	0.17	7.6
NaCl	0.40	1.33	0.12	7.6
NaCl	0.20	0.73	0.08	7.7
NaCl	0.09	0.30	0.04	6.7
$NaNO_3$	0.78	2.80	0.13	7.3
$NaNO_3$	0.20	1.35	0.09	6.7
$NaNO_3$	0.03	0.41	0.03	6.7
Na_2SO_4	0.99	3.14	0.20	7.1
Na_2SO_4	0.17	1.84	0.17	7.1
Na_2SO_4	0.09	0.46	0.14	7.0

[a] Initial conditions: $m_{steel\ wool}$ = 2 g/L; pH_{ini} = 7.0, air flow = 0.8 L/min.
[b] Relative standard deviations for replicate runs were smaller than 8% (n = 4).

an engineering viewpoint this suggests that for long-term reactors, steel wool loadings should be well above the cutoff value (6 m^2 for the conditions of this study) in order to prevent the corrosion rates from being controlled by decreasing contact areas owing to the exhaustion of iron fillings.

3.3. Effect of dissolved salts

In some regions, natural groundwater sources may have large amounts of dissolved ions that may vary with seasonal conditions and population demands. Since the presence of dissolved salts may influence iron corrosion rates, a set of experiments was performed exposing identical amounts of steel wool to solutions of different initial electrolyte concentrations. Although differences in the $Fe(III)_{tot}$ profiles were observed at early reaction stages, in all cases steady production profiles were achieved after 30 min. As shown in Table 1, the steady rates of $Fe(III)_{tot}$ production increase with the solution conductivity within the analyzed ranges.

Interestingly, the measured concentration of NO_3^- remained constant within the analyzed timescale, indicating that the reduction of NO_3^- by Fe(0) is negligible during our experiments. It should also be mentioned that the rates observed in the presence of Cl^- are somewhat higher than the ones observed with NO_3^- but lower than the ones measured with SO_4^{-2}, thus pitting corrosion due to the ability of Cl^- to destabilize ferric oxides seems to play a secondary role in the studied experimental domain.

In agreement with the dependence on the contact area observed for corrosion product generation, the increase of $Fe(III)_{tot}$ production rates with the solution conductivity confirms that the rate-controlling processes for the overall oxidation are of electrochemical nature. Hence, at high electrolyte concentrations the charge transport between anodic sites (wherein Fe(0) oxidation takes place) and cathodic sites (where both H_2O and O_2 reductions take place) increases, thus promoting the electrochemical corrosion of ZVI [7,19,20].

Biterna et al. have recently reported [33] the effect of several anions on the removal of arsenate by ZVI. They found an acceleration of arsenate removal in the presence of several ions including chloride, nitrate and sulfate in concentrations similar to the ones reported in the present study. Their results for As removal could likely be explained, at least partially, by taking into account the increase in ZVI corrosion rates.

3.4. Distribution of corrosion products

Preliminary adsorption experiments conducted in our laboratory showed that freshly prepared colloidal particles (≈30 min) are more efficient for As removal than aged particles (≈30 days). Therefore, studies concerning the behavior of colloidal iron oxyhydroxides produced in situ are relevant since treatment facilities based on the short-timescale interaction between nascent particles and arsenic species may be advantageous in some specific cases.

Several authors have reported the formation of a passive oxide layer on the iron surface that mediates iron corrosion [4,7], and it is known that the nature of this corrosion coating is critical in the observed ZVI reactivity [12]. In addition, it has been proposed [19,20] that the spatial relationship between Fe(0) surfaces and corrosion products, rather than the overall quantity of corrosion products, determines the reactivity of ZVI. Therefore, two different experimental approaches were taken in order to analyze the distribution of suspended particles produced by steel wool corrosion inside the batch reactor.

The first experiment compared the $Fe(III)_{tot}$ profiles obtained with and without stirring (Fig. 3). Linear $Fe(III)_{tot}$ profiles were observed in both cases during the first 60 min. However, for longer elapsed times, the $Fe(III)_{tot}$ profiles for the unstirred system showed a clear bend until [$Fe(III)_{tot}$] reached a constant value, whereas the $Fe(III)_{tot}$ profiles for the stirred system remained linear. It is worth mentioning that in both cases the steel wool was free of a visible oxidized layer and retained its characteristic metallic glaze even after more than 8 h. These results differ from those obtained by Zhang and Huang [24] who reported the formation of a visible brownish coating during the first 3 h, which turned black after 6 h. Hence, for the conditions tested, the steel wool used in the present work behaves differently.

In order to clarify the behavior observed for the unstirred systems, a second experiment was conducted. The $Fe(III)_{tot}$ produced by the same steel wool sample was measured in an unstirred system for 300 min by replacing the liquid phase every 60 min (Fig. 3, inset). The profiles of $Fe(III)_{tot}$ obtained during the different cycles did not show significant differences, suggesting that even for the unstirred systems the reactivity of steel wool is not influenced by the accumulation of corrosion products.

The above results indicate that the curvature in $Fe(III)_{tot}$ profiles in the unstirred system can be attributed to a sampling effect. For periods longer than 60 min, a nonuniform distribution of suspended particles is established inside the unstirred batch reactor. This phenomenon can be associated with the enhancement in the particle sedimentation rates that accompanies the increase of particle size due to maturation and growth [16]. Thus, the plateau in $Fe(III)_{tot}$ concentration is related to a stationary state of production/sedimentation of corrosion particles achieved for aging periods longer than 60 min.

It is worth pointing out that the absence of a visible corrosion coating on the steel wool surface indicates that the formation of colloidal corrosion particles in our system could be more likely asso-

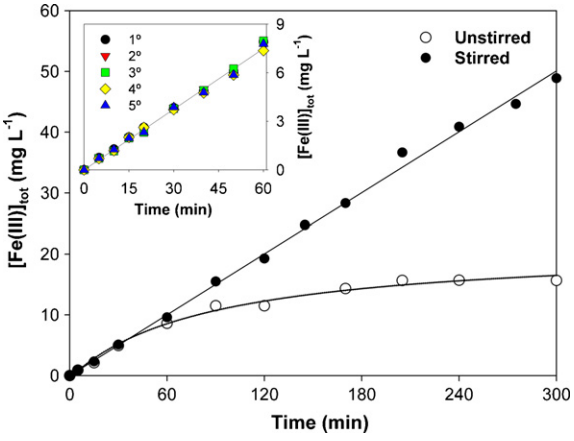

Fig. 3. [$Fe(III)_{tot}$] profiles measured with and without stirring. Conditions: tap water; σ_{ini} = 820 μS/cm; pH_{ini} = 7.2; air flow = 0.8 L/min; $m_{steel\ wool}$ = 3 g/L.

ciated with homogeneous processes (either in the neighborhood of the ZVI/solution interface or in the bulk solution) rather than with the stripping of surface oxides from mechanical abrasion. It has been suggested [19] that oxygenated, high ionic strength solutions promote the formation and stabilization of ferrihydrite clusters away from Fe(0) surfaces [20], whereas anoxic corrosion promotes the formation of magnetite films that passivate the Fe(0) surface. Thus, depending on the ZVI source and the reaction conditions used, the homogeneous formation of colloidal particles should not be disregarded and deserves special attention for designing efficient reactors. In the particular case of batch systems, vigorous stirring should be applied since a proper distribution of suspended oxyhydroxides will reduce mass transfer limitations (i.e., arsenic species to the adsorption sites and molecular oxygen to the corrosion sites).

3.5. Effect of pH

A number of studies have reported the effect of pH on the uptake of arsenic species in ZVI systems [2,6,26,27]. In addition, the pH effect on the removal of arsenic species by iron oxides and iron hydroxides is well established [4,28,29], whereas only a few papers [2,6] have addressed the effect of pH on iron corrosion rates at circumneutral conditions within the framework of the ZVI technique for As removal. Therefore, we tested $Fe(III)_{tot}$ production rates by steel wool under continuous air supply in the pH range 3.5–10.0. The rates of total Fe(III) production as a function of the initial pH showed a broad maximum for values comprised between 6 and 8 (Fig. S3, Sup. Mat.). Besides, the final pH values obtained after 60 min were very similar for the whole set. It is worth emphasizing that these results are important from a technological point of view since although iron corrosion rates strongly depend on the pH, $Fe(III)_{tot}$ production rates are practically constant within the usual pH range of drinking water.

3.5.1. $Fe(II)_{tot}$ and $Fe(III)_{tot}$ production

As previously noticed by Noubactep [30], the pH dependence of the iron corrosion mechanism is usually overlooked in the literature about ZVI technology, since two different processes may contribute to the corrosion of iron: "the hydrogen evolution mechanism" and "the oxygen adsorption mechanism." Hence, in order to characterize some key features of steel wool corrosion, additional experiments were conducted both in the absence and in the presence of dissolved oxygen at pH 3.5, 7.0 and 9.0. Table 2 shows the steady values of pH and $[Fe(II)_{tot}]$ achieved after 45 min of reaction time as well as the initial rates of iron species production.

3.5.1.1. N_2-purged experiments. For the N_2-purged experiment initiated in alkaline media, the pH remained constant and no Fe(II) production was detected in the analyzed timescale. On the other hand, the anoxic test started in neutral media showed a fast pH shift of one unit within the first 10 min and then remained constant. Besides, a rather small amount of total Fe(II) was produced within the first 10 min, and then ferrous iron production stopped. These results indicate that corrosion does not take place at an appreciable rate in the absence of dissolved oxygen at pH values higher than 7.5.

During the experiment initiated in acid conditions, a noticeable pH increase was accompanied by the formation of Fe(II) during the first 60 min. After this time period, both the pH and Fe(II) concentration reached constant values. Noteworthy, the steel wool surface retained its metallic glaze, and the analysis of $Fe(II)_{tot}$ and $Fe(II)_{filt}$ fractions yielded identical values within experimental error, suggesting that Fe(II) precipitation (R6) has a minor contribution in the studied pH range. In addition, no Fe(III) was detected in any of the experiments conducted with N_2-purged solutions, which is in line with the results discussed in Section 3.1.1.

Consequently, in agreement with previous studies [12], the above results show that the contribution of reaction (R1) to the continuous production of species for arsenic uptake at circumneutral pH is negligible unless dissolved oxygen is severely exhausted. In such case, Fe(II) production occurs at a much lower rate. It is also important to point out that while the analysis of Fe(II) fractions indicates that reaction (R6) may be neglected for N_2-purged solutions, in the presence of dissolved oxygen the co-precipitation/adsorption of Fe(II) species with/on nascent particles should not be completely ruled out.

3.5.1.2. Air-purged experiments. Although a wide range of initial pH conditions was tested, the steady pH values obtained under continuous air supply are very close, especially for the experiments started in neutral and alkaline media. The pH increase recorded under acidic and neutral conditions is in agreement with the results previously reported by other authors in ZVI systems for arsenic removal [4,5]. It is also observed that the concentration of Fe(II) is strongly pH dependent, being much higher for the acid experiment. This difference is at least partially related to the pH dependence of Fe(II) oxidation rates [18,31,34].

The pH profiles showed a slight increase for the experiment initiated at neutral conditions and a small decrease for the experiment initiated at pH 9.0. As for the N_2-purged test, an important pH increase is accompanied by the production of Fe(II) species in the experiment initiated in acid medium. However, in contrast with the oxygen-free experiment, significant amounts of Fe(III) are also produced.

The inspection of Table 2 values shows that the rates of ZVI oxidation decrease when the initial pH is increased; a similar behavior has been previously reported [6]. Since for pH values between 7 and 9 the contribution of anoxic corrosion may be neglected within the spanned timescale, the latter result suggests that oxygen-mediated iron corrosion also decreases with increasing pH in the analyzed range.

3.5.2. pH evolution

The pH profiles observed with different initial $[H^+]$ values and dissolved oxygen concentrations can be qualitatively explained using the reaction scheme presented in the introduction. For the experiments initiated in acid media, the oxidation of one mole of metallic iron mediated by both water and dissolved oxygen ((R1) and (R2)) is accompanied by the production of two moles of HO^- and one mole of Fe(II) ions. In addition, in the presence of dissolved oxygen, the oxidation of ferrous species yields an additional HO^- (R4). The aforementioned processes allow explaining the differences in the observed initial rates of pH increase (Fig. S4, Sup. Mat.) since for the N_2-purged experiment only (R1) contributes to HO^- generation, whereas in the presence of oxygen the faster pH increase is related to the contribution of two additional reactions (i.e., (R2) and (R4)).

However, the constant pH values reached in both N_2-purged and air-saturated solutions are associated with two distinct phenomena. In the absence of dissolved oxygen, Fe(II) production continues until pH values wherein water-mediated iron oxidation rates are negligible (R1), then both $Fe(II)_{tot}$ and pH values remain constant with time. On the contrary, in the presence of dissolved oxygen the oxidation of Fe(II) to Fe(III) (R4) is coupled with the generation of a third mole of HO^- per mole of oxidized ZVI. While the rate of Fe(II) oxidation increases with the pH increase [18,31,34] and the resulting ferric species are quickly hydrolyzed yielding 3 moles of H^+ per mole of Fe(III) (R5), steady-state values for both $[Fe(II)]_{filt}$ and $[HO^-]$ are attained when their rates of production by redox reactions are balanced with their rates of consumption through redox and precipitation processes. A simple kinetic analysis further supports the

Table 2
Effect of pH on steel wool corrosion[a,b].

pH_{ini}	pH_{steady}	$[Fe(II)_{tot}]_{steady}$ (mg/L)	$r^{ini}_{Fe(II)tot}$ (mg/L min)[c]	$r^{ini}_{Fe(III)tot}$ (mg/L min)[c]
Anaerobic conditions				
3.00	7.80	7.6	0.73	–
7.00	8.05	0.8	0.08	–
9.00	9.00	n.d.[d]	–	–
Aerobic conditions				
3.50	6.45	24.4	1.37	0.24
7.05	7.65	3.4	0.42	0.31
9.00	8.05	3.4	0.08	0.26

[a] $r^{ini}_{Fe(II)tot}$ = initial rate of $Fe(II)_{tot}$ production; $r^{ini}_{Fe(III)tot}$ = initial rate of $Fe(III)_{tot}$ production.
[b] Initial conditions: synthetic water; σ_{ini} = 1700 μS/cm; $m_{steel\ wool}$ = 3.4 g/L; gas flow = 0.8 L/min (N_2 or air).
[c] Replicate runs showed good reproducibility, the relative standard deviations being smaller than 7% in all cases (n = 3).
[d] n.d. = not detected.

latter hypothesis. The $Fe(II)_{aq}$ concentration is governed by Eq. (1)

$$\frac{d[Fe(II)_{aq}]}{dt} = r_{Prod} - k_{R4} \times [Fe(II)_{aq}] \times [HO^-]^2 \times pO_2 \quad (1)$$

where r_{Prod} represents the rate of Fe(II) production through the parallel pathways of ZVI oxidation, while the second term shows the reported rate law for (R4) [18,34]. Assuming $d[Fe(II)]/dt \approx 0$, the steady pH value can be roughly estimated. By combining $k_{R4} \approx 8.0 \times 10^{13}$ min^{-1} atm^{-1} mol^{-2} L^2 [31] with the values presented in Table 2, an estimation of 6.67 is obtained for the steady pH value recorded during the experiment started in acidic media. Although the predicted value differs from the observed one (6.45), it should be pointed out that the values reported in Table 2 correspond to total Fe(II) and that several interfacial phenomena [31,34], which have not been taken into account in this simple model, may also be involved.

The small pH increase observed for the experiment initiated at pH 7.0 in air-saturated systems can be explained using the same argumentation. On the other hand, the small decrease in pH observed for the aerobic test initiated at pH 9.0 might be ascribed to the formation of $Fe(HO)_4^-$, which is the dominant soluble iron species at pH > 8.5 [14]. Thus, three moles of HO^- are produced per mole of Fe(0) oxidized to Fe(III), but four moles of HO^- would be consumed in the formation of $Fe(HO)_4^-$.

It is worth mentioning that other authors have discussed the buffering effects of Fe(II), Fe(III) and inorganic carbon in ZVI systems [25,32]. Since the steady pH value reached in the N_2-purged experiment is related to the inhibition of steel wool corrosion and we observed no differences in blank experiments performed with solutions free from inorganic carbon species, the buffering effects of both Fe(II) and $CO_{2(aq)}/HCO_3^-$ may be neglected in our conditions. Consequently, our results show that the complex pH evolution observed is linked to the combination of redox and Fe(III) precipitation reactions, rather than to the contribution of a single buffering process.

Thus, the dependence on the initial pH of average $Fe(III)_{tot}$ production rates discussed at the beginning of this section is related to two factors. On the one hand, the relative small differences in the observed rates may be attributed to the pH evolution since for oxygen-saturated solutions the initial pH quickly shifts towards circumneutral values. On the other hand, the interplay of the opposite dependencies of Fe(0) and Fe(II) oxidation rates on the pH may explain the observed maximum since the oxidation of Fe(0) decreases with pH increase (Table 2), whereas Fe(II) oxidation rates increase with pH.

3.6. Effect of the presence of arsenic species on iron corrosion

Previous studies on ZVI systems for As removal [7,8] have established that arsenic species may play a significant role as corrosion inhibitors. Therefore, we conducted a set of experiments comparing the release of iron species in the presence of As(V) or As(III) in both acidic and basic media. Table 3 compares concentrations of iron species measured for a set of ZVI corrosion experiments performed at different initial pH values, in the absence and in the presence of As(III) or As(V) species.

In acid solutions, As(III) inhibits about 70% the release of iron species, whereas As(V) has a minimal effect. On the other hand, the concentrations obtained in alkaline media clearly show that As(III) and As(V) markedly decrease the rates of metallic iron oxidation since in both cases an inhibition of more than 80% is observed. It has been reported that removal of As(V), by both adsorption onto Fe oxides [4] and co-precipitation with Fe(III) [28], decreases from pH 5.5 to pH 9, whereas removal of As(III) increases in the same range. Table 3 results clearly show that the pH dependence observed for arsenic uptake in ZVI systems is not only associated with different removal properties of the iron oxyhydroxides, but also with the influence of arsenic species on the rates of corrosion product release.

In addition to surface adsorption, precipitation and co-precipitation processes [35], redox reactions such as As(V) or As(III) reduction and As(III) oxidation may play a role in ZVI/As systems. Although it is known that Fe(0) can reduce As(V) to As(III) and As(0)

Table 3
Effect of arsenic species on iron species concentrations[a,b,c].

Conc. given in mg/L	Initial pH = 5.5			Initial pH = 8.5		
	Blank	As(III)	As(V)	Blank	As(III)	As(V)
$[Fe(II)_{filt}]$	2.06	1.20	1.53	0.58	n.d.[d]	0.34
$[Fe(II)_{tot}]$	5.85	1.67	3.77	2.32	0.61	1.05
$[Fe(III)_{tot}]$	15.8	4.75	15.3	15.7	1.72	2.52
$[Fe(II)_{tot}] + [Fe(III)_{tot}]$	21.6	6.42	19.1	18.0	2.33	3.57

[a] Values measured at 75 min.
[b] Initial conditions: $[As]_0$ = 1 mg/L; tap water; σ_{ini} = 1700 μS/cm; $m_{steel\ wool}$ = 3.4 g/L; air flow 0.8 L/min.
[c] The reported results are the mean of 3 replicated measurements.
[d] n.d. = not detected.

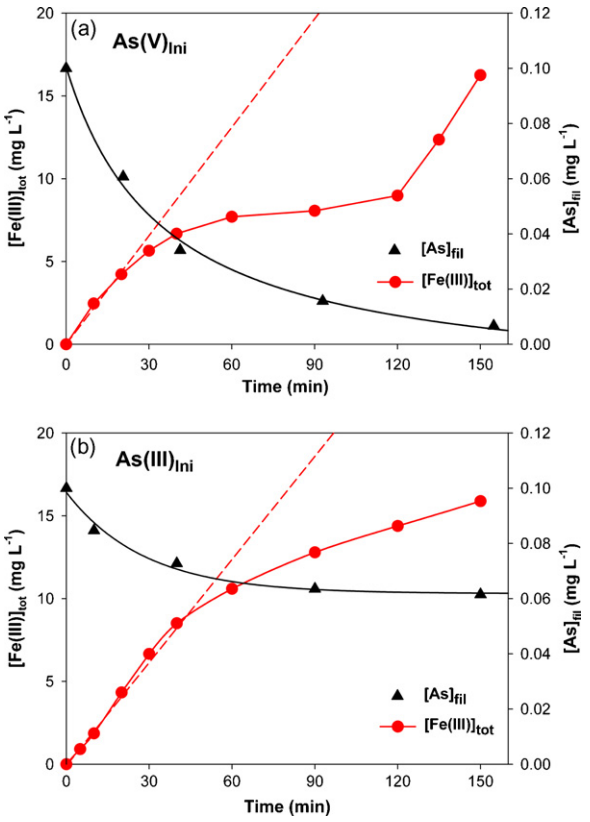

Fig. 4. $Fe(III)_{tot}$ production profiles obtained in the absence and in the presence of As(V) or As(III). Conditions: synthetic water; σ_{ini} = 1.50 mS/cm; pH_{ini} = 7.1; air flow = 0.8 L/min; $m_{steel\ wool}$ = 3 g/L. Solid lines show profiles observed in the presence of As(V) or As(III), dashed lines show profiles in the absence of arsenic.

[2], for the timescales analyzed in the present work these processes are probably too slow to be important. On the other hand, the co-oxidation of Fe(II) and As(III) in the presence of dissolved oxygen [3,5,9] may be important in our experimental conditions. Since the amount of dissolved oxygen consumed by As(III) will depend on the ratio [As(III)]/[Fe(II)] [3], the performance of a removal process may be dramatically affected by the arsenic levels in the contaminated waters. In particular, As(III) species may deplete dissolved oxygen in the neighborhood of the ZVI/suspension interface, where the concentration of Fe(II) is expected to be high. In addition, as discussed in Section 3.5, the oxidation of Fe(II) is one of the main factors controlling the pH evolution, so the above-mentioned redox processes may affect the steady value of pH reached in these experiments.

In order to gain insight into the correlation between arsenic and ferric species production, the concentration profiles of arsenic and $Fe(III)_{tot}$ were analyzed in a set of corrosion experiments started at pH 7.0 under aerobic conditions. Fig. 4 compares the production of $Fe(III)_{tot}$ in the presence (solid lines) and in the absence (dashed lines) of arsenic species.

In the presence of penta-valent arsenic, $Fe(III)_{tot}$ concentration quickly deviates from the profile observed in arsenic-free solutions, the rate of corrosion being about 90% slower. However, as the concentration of soluble As(V) decreases, the rate of $Fe(III)_{tot}$ production increases and after 120 min the concentration profile exhibits a slope similar to the one obtained in arsenic-free solutions. This result indicates that once As(V) has been removed, ZVI corrodes at the rate observed in the absence of arsenic.

A different behavior is observed in the presence of trivalent arsenic since during at least the first 40 min the production of $Fe(III)_{tot}$ is equal to or slightly higher than the one observed in arsenic-free solutions. Subsequently, $Fe(III)_{tot}$ production decreased about 75% and at the same time soluble arsenic concentration reached a plateau, the removal efficiency being only 38%. In addition, the absence of recovery in the $Fe(III)_{tot}$ production rate within the analyzed time window may be related to the high residual arsenic concentration.

While several features of corrosion inhibition mechanisms by As(V) and As(III) species remain unclear, the results of the present study show that there is a strong interaction between iron species and arsenic anions that prevents the release of colloidal corrosion particles to the bulk solution. More research is needed in order to ascertain the mechanism of corrosion inhibition.

4. Conclusions

- The simultaneous analysis of the oxidation states observed for total and filterable iron fractions allows drawing useful conclusions concerning the corrosion mechanism. The experiments conducted in oxygen-free solutions showed that the mechanism of steel wool oxidation that is linked to H_2 evolution (R1) is only capable of yielding Fe(II) species at low rates and becomes negligible at circumneutral pH values unless dissolved oxygen is severely exhausted. In addition, the analysis of Fe(II) fractions indicates that the processes represented by (R6) may also be neglected for N_2-purged solutions. However, in the presence of dissolved oxygen the co-precipitation/adsorption of Fe(II) species with/on nascent particles should not be completely ruled out.
- In the presence of dissolved oxygen, Fe(II) concentration achieves a steady state where the rate of $Fe(III)_{tot}$ generation is determined by the rate of Fe(0) oxidation. The increase of corrosion rates with both contact area and solution conductivity further indicates that the rate-controlling step for the overall processes is a heterogeneous oxidation of electrochemical nature. In addition, the inhomogeneous distribution of dissolved oxygen is important from a technological perspective since mass transport limitations may have a critical impact on ZVI corrosion rates.
- The distribution of corrosion products is strongly dependent on the ZVI source. A visible corrosion layer was observed with lost head nails but not in the case of steel wool. This latter result indicates that the formation of colloidal particles from steel wool is more likely associated with homogeneous processes (either in the neighborhood of the ZVI/solution interface or in the bulk solution) rather than with the stripping of surface oxides from mechanical abrasion. Thus, depending on the ZVI source and the reaction conditions used, the homogeneous formation of particles should not be disregarded and deserves special attention for designing efficient reactors.
- The production of $Fe(III)_{tot}$ after 60 min is practically constant for initial pH values comprised within the usual range of drinking water. The complex pH evolution observed is related to the combination of redox and precipitation reactions, rather than to the contribution of a single process. Besides, the interplay of the opposite dependencies of Fe(0) and Fe(II) oxidation rates on the pH may explain the observed maximum since oxidation of Fe(0) decreases with pH increase, whereas Fe(II) oxidation rates increase with pH.
- The results of the present study show that there is a strong interaction between iron species and arsenic anions that prevents the release of colloidal corrosion particles to the bulk solution. This inhibition effect is dependent on the solution pH and the arsenic oxidation state.

Acknowledgements

The authors wish to thank the Laboratorio de Ingeniería Sanitaria de la Facultad de Ingeniería de la Universidad Nacional de

La Plata (Argentina) for the financial support of this research. F. S. García Einschlag and A. Porta are members of the research career of CONICET and CIC-PBA, respectively. We are greatly indebted to the reviewers for their critical comments and suggestions which improved the quality of the manuscript.

Appendix A. Supplementary data

Supplementary data associated with this article can be found, in the online version, at doi:10.1016/j.cej.2009.01.029.

References

[1] J.F. Ferguson, J. Garvis, Review of arsenic cycle in natural waters, Water Res. 6 (1972) 1259–1274.
[2] S. Bang, M.D. Johnson, G.P. Korfiatis, X. Meng, Chemical reactions between arsenic and zero-valent iron in water, Water Res. 39 (2005) 763–770.
[3] L.C. Roberts, S.J. Hug, T. Ruettimann, M. Billah, A.W. Khan, M.T. Rahman, Arsenic removal with iron(II) and iron(III) waters with high silicate and phosphate concentrations, Environ. Sci. Technol. 38 (2004) 307–315.
[4] C. Su, R. Puls, Arsenate and arsenite removal by zero valent iron: kinetics, redox transformation and implications for in situ groundwater remediation, Environ. Sci. Technol. 35 (2001) 1487–1492.
[5] O.X. Leupin, S.J. Hug, Oxidation and removal of arsenic(III) from aereated groundwater by filtration through sand and zero valent iron, Water Res. 39 (2005) 1729–1740.
[6] S. Bang, G.P. Korfiatis, X. Meng, Removal of arsenic from water by zero-valent iron, J. Hazard. Mater. 121 (2005) 61–67.
[7] N. Melitas, J.P. Wang, M. Conklin, P. O'Day, J. Farrell, Understanding soluble arsenate removal kinetics by zero valent iron, Environ. Sci. Technol. 36 (2002) 2074–2081.
[8] J. Farrell, J. Wang, P. OïDay, M. Conklin, Electrochemical and spectroscopy study of arsenate removal from water using zero valent iron media, Environ. Sci. Technol. 35 (2001) 2026–2032.
[9] R.B. Johnston, P.C. Singer, Redox reactions in the Fe–As–O_2 system, Chemosphere 69 (2007) 517–525.
[10] J.A. Lackovic, N.P. Nikolaidis, G.M. Dobbs, Inorganic arsenic removal by zero valent iron, Environ. Eng. Sci. 17 (2000) 29–39.
[11] B. Manning, M.L. Hunt, C. Amrhein, J.A. Yarmoff, Arsenic(III) and arsenic(V) reactions with zero valent iron corrosion products, Environ. Sci. Technol. 36 (2002) 5455–5461.
[12] T.C. Zhang, Y.H. Huang, Profiling iron corrosion coating on iron grains in a zero valent iron system under the influence of dissolved oxygen, Water. Res. 40 (2006) 2311–2320.
[13] K. Tyravola, N.P. Nikolaidis, N. Veranis, N. Kallithrakas-Kontos, P.E. Koulouridakis, Arsenic removal from geothermal water with zero-valent iron – effect of temperature, phosphate and nitrate, Water. Res. 40 (2006) 2375–2386.
[14] A.N. Pham, A.L. Rose, A.J. Fetiz, T.D. Waite, Kinetics of Fe(III) precipitation in aqueous solution at pH 6.0–9.5 and 25 °C, Geochim. Cosmochim. Acta 70 (2006) 640–650.
[15] A.L. Rose, T.D. Waite, Kinetics of hydrolysis and precipitation of ferric iron in seawater, Environ. Sci. Technol. 37 (2003) 3897–3903.
[16] Y. Deng, Formation of iron(III) hydroxides from homogeneous solutions, Water Res. 31 (1997) 1347–1354.
[17] B. Park, B.A. Dempsey, Heterogeneous oxidation of Fe(II) on ferric oxide at neutral pH and low partial pressure of O_2, Environ. Sci. Technol. 39 (2005) 6494–6500.
[18] W. Stumm, F. Lee, Oxygenation of ferrous iron, Ind. Eng. Chem. 53 (1961) 143.
[19] Y. Furukawa, J.-W. Kim, J. Watkins, R.T. Wilkin, Formation of ferrihydrite and associated iron corrosion products in permeable reactive barriers of zero-valent iron, Environ. Sci. Technol. 36 (2002) 5469–5475.
[20] J. Farrell, M. Kason, N. Melitas, T. Li, Investigation of the long-term performance of zero-valent iron for reductive dechlorination of trichloroethylene, Environ. Sci. Technol. 34 (2000) 514–521.
[21] D. Mishra, J. Farrell, Evaluation of mixed valent iron oxides as reactive adsorbents for arsenic removal, Environ. Sci. Technol. 39 (2005) 9689–9694.
[22] M. Rios-Enriquez, N. Shahin, C. Durán-de-Bazúa, J. Lang, E. Oliveros, S.H. Bossmann, A.M. Braun, Optimization of the heterogeneous fenton-oxidation of the model pollutant 2,4-xylidine using the optimal experimental design methodology, Solar Energy 77 (2004) 491–501.
[23] Standard Method, Standard Methods for the Examination of Water and Wastewater, 20th ed. American Water Works Association (AWWA), American Public Health Association, American Water Works Association and Water Environment Federation, Part 3000 Metals, 3500 – As B, Silver Diethyldithiocarbamate Method, 3-60–3-61, 1998.
[24] Y.H. Huang, T.C. Zhang, Effect of dissolved oxygen on formation of corrosion products and concomitant oxygen and nitrate reduction in zero-valent iron systems with or without aqueous Fe^{2+}, Water Res. 39 (2005) 1751–1760.
[25] Y.H. Huang, T.C. Zhang, Reduction of nitrobenzene and formation of corrosion coatings in zero valent iron system, Water Res. 40 (2006) 3075–3082.
[26] H. Sun, L. Wang, R. Zhang, J. Sui, G. Xu, Treatment of groundwater polluted by arsenic compounds by zero valent iron, J. Hazard. Mater. B129 (2006) 297–303.
[27] C. Su, R.W. Puls, Arsenate and arsenite removal by zero valent iron: effect of phosphate, silicate, carbonate, borate, sulfate, chromate, molybdate, and nitrate, relative to chloride, Environ. Sci. Technol. 35 (2001) 4562–4568.
[28] X. Meng, S. Bang, G.P. Korfiatis, Effect of silicate, sulfate and carbonate on arsenic removal by ferric chloride, Water Res. 34 (2000) 1255–1261.
[29] Y. Jia, L. Xu, Z. Fang, G.P. Demopoulos, Observation of surface precipitation of arsenate on ferrihydrite, Environ. Sci. Technol. 40 (2006) 3248–3253.
[30] C. Noubactep, Comments on "Comparison of reductive dechlorination of *p*-chlorophenol using Fe^0", J. Hazard. Mater. 148 (2007) 775–777.
[31] J. Buffle, R.R. De Vitre, Chemical and Biological Regulation of Aquatic Systems, CRC Press, Inc. Company, Lewis Publishers, USA, 1994, 14 pp. (Chap. 3).
[32] A.J. Feitz, S.H. Joo, J. Guan, Q. Sun, D.L. Sedlak, T.D. Waite, Oxidative transformation of contaminants using colloidal zero-valent iron, Colloids and Surfaces A: Physicochem. Eng. Aspects 265 (2005) 88–94.
[33] M. Biterna, A. Arditsoglou, E. Tsikouras, D. Voutsa, Arsenate removal by zero valent iron: batch and column tests, J. Hazard. Mater. 149 (2007) 548–552.
[34] N. El Azher, B. Gourich, C. Vial, M. Belhaj Soulami, M. Ziyad, Study of ferrous iron oxidation in Morocco drinking water in an airlift reactor, Chem. Eng. Process. 47 (2008) 1877–1886.
[35] H.-L. Lien, R.T. Wilkin, High-level arsenite removal from groundwater by zero-valent iron, Chemosphere 59 (2005) 377–386.
[36] S. Kundu, A.K. Gupta, As(III) removal from aqueous medium in fixed bed using iron oxide-coated cement (IOCC): experimental and modeling studies, Chem. Eng. J. 129 (2007) 123–131.